

Reply to Anonymous Referee #1

Kai Zhang (kai.zhang@pnnl.gov)
Pacific Northwest National Laboratory

We thank the referee for the helpful and constructive comments. Our responses are detailed below.

This manuscript describes a method to estimate subgrid scale variability of surface winds in the global model CAM5 to improve the computation of dust and sea salt emission fluxes. The approach builds upon previous work by various authors. The authors describe a method to quantify wind variability due to small-scale processes like turbulence, and describe the surface wind speeds in terms of a Weibull probability distribution. The global model is modified accordingly and changes in sea salt and dust emissions and distributions are compared to the standard setup.

Parameterization of subgrid scale variability for modelling wind-driven emission of primary aerosol particles is a relevant topic, and the authors present an interesting method how a quantification of the such processes can be achieved. They find that while sea salt aerosol emissions are not substantially changed by subgrid scale wind variability, the changes in dust emission can be important. However, the authors should address several issues in a revised version.

Comment: A major problem is the lack of an appropriate evaluation of the model results using the new wind parameterization used for computing primary aerosol emissions. In section 5.2 a comparison of averaged model results with MISR optical thickness retrievals is shown as sole evaluation of the model results. While the MISR aerosol product is certainly well established and useful, there are undoubtedly more observations that should be used for the model evaluation. E.g., Huneus et al. (2011, ACP) the results from global dust models are compared to standard dust datasets. Evaluation of dust model results with AOD from the AERONET sunphotometer network, in particular the 'coarse mode' aerosol, is a standard method even for global models. Not only annual mean values of model results and observations should be compared, but also time series for different locations. Even if no 1:1 relationship can be expected between model results and observations given the difficulties comparing a model grid value with a point measurement, at least such comparisons can indicate if the new results (e.g. EXP4 vs. Control) improve the model agreement with observations, e.g. in terms of seasonality and regional differences.

Reply: Evaluation is indeed a major challenge of this study due to the lack of direct observation of sea salt and dust emissions on the global scale. The AERONET AOD data are limited in their spatial and temporal coverage when dust is the species of interest. We have selected AERONET sites near dust source regions and compared high-frequency AOD measurements with model simulations in the format of scatter plots, time series, and frequency distributions. It turns out the measurements that

fall in our simulation period are located in regions where the CTRL simulation and the modified model (EXP4) give very similar annual mean dust AOD (Figure R1.1). The frequency distributions (Figure R1.2) and seasonal cycles (Figure R1.3 and R1.4) are also very similar. These figures are not included in the paper because they do not indicate systematic improvement or degradation of model fidelity. In dust source regions where CTRL and EXP4 do give considerably different AOD (Taklamakan Desert, Southeast Iran, and Pakistan), there are unfortunately no AERONET data in the year 2006, and only a few days of measurements in the other years. In the future it would be useful to find other sources of observational data to evaluate the simulations in those regions.

A paragraph is added to the revised manuscript at the end of Section 5.4, "Comparison with AOD observations":

"In addition to MISR, we have compared the simulated AOD with high-frequency measurements from the Aerosol Robotic Network (AERONET) sites close to the dust source regions. It turns out that the AERONET measurements falling in our simulation period are located in regions where CTRL and EXP4 give very similar dust AOD. The comparison thus did not indicate systematic improvement or degradation in terms of the agreement between model results and measurements. In the Taklamakan Desert, Southeast Iran, and Pakistan where AOD in EXP4 is considerably higher than that in CTRL (Fig. 18), it is not yet known how the two simulations compare with observations due to the unfortunate lack of data."

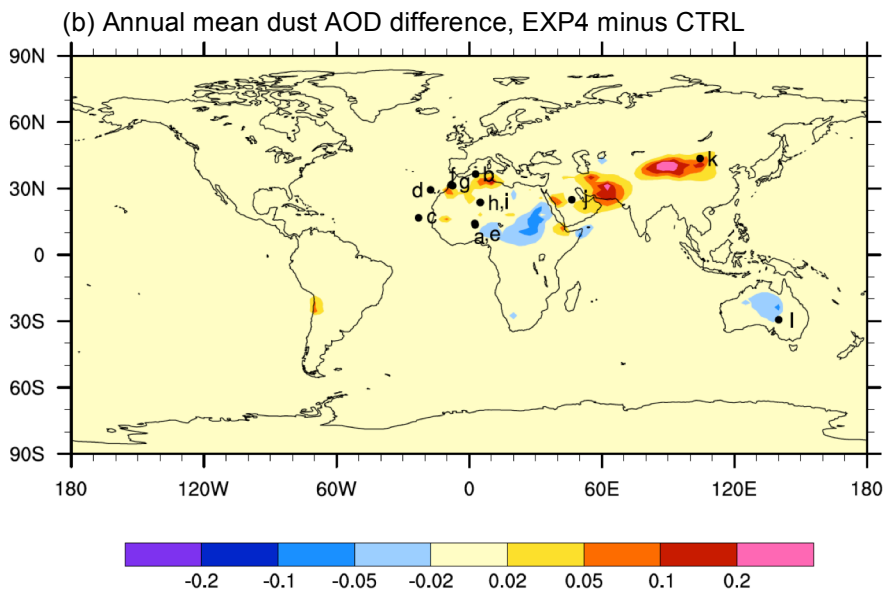
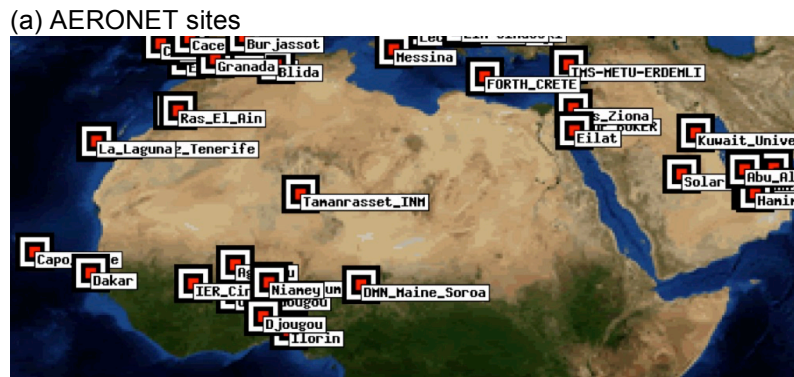


Figure R1.1 (a) AERONET sites in or near North Africa that have measurements available for the year 2006. (b) Simulated annual mean AOD differences between EXP4 and CTRL of the year 2006. The black marks and the labels indicate locations of the AERONET sites where observed and modeled AOD are compared in Figures R1.2, R1.3, and R1.4 below.

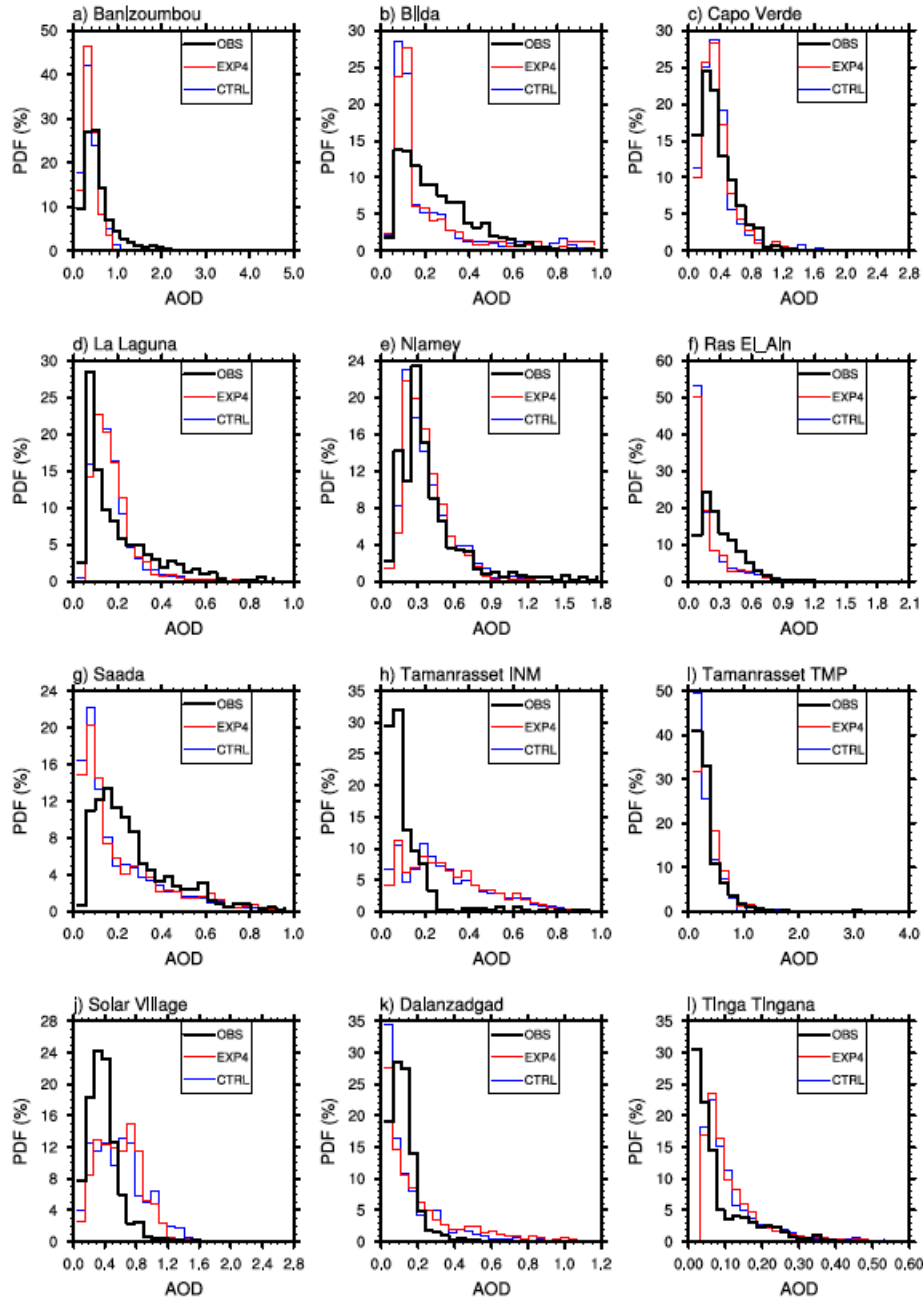


Figure R1.2. Frequency distributions of measured and simulated hourly AOD at the 12 AERONET sites indicated in Figure R1.1. Both measurements and simulations are from the year 2006. Model results are masked out when the AERONET measurements are missing.

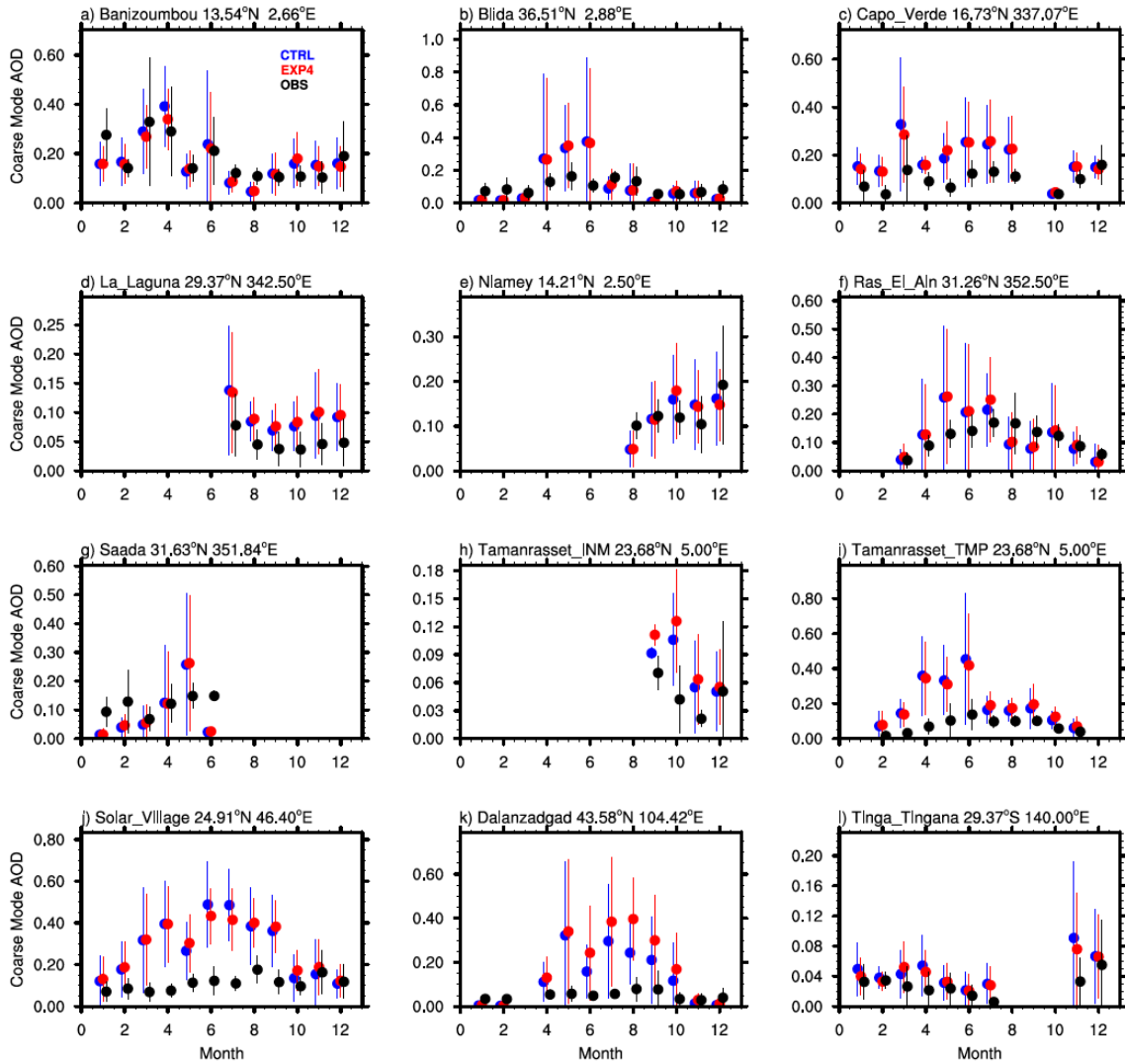


Figure R1.3: Observed and simulated monthly mean *total* AOD at 12 AERONET sites indicated in Figure R1.1. The error bars indicate ± 1 standard deviations of hourly AOD. Model results are masked out when the AERONET measurements are missing.

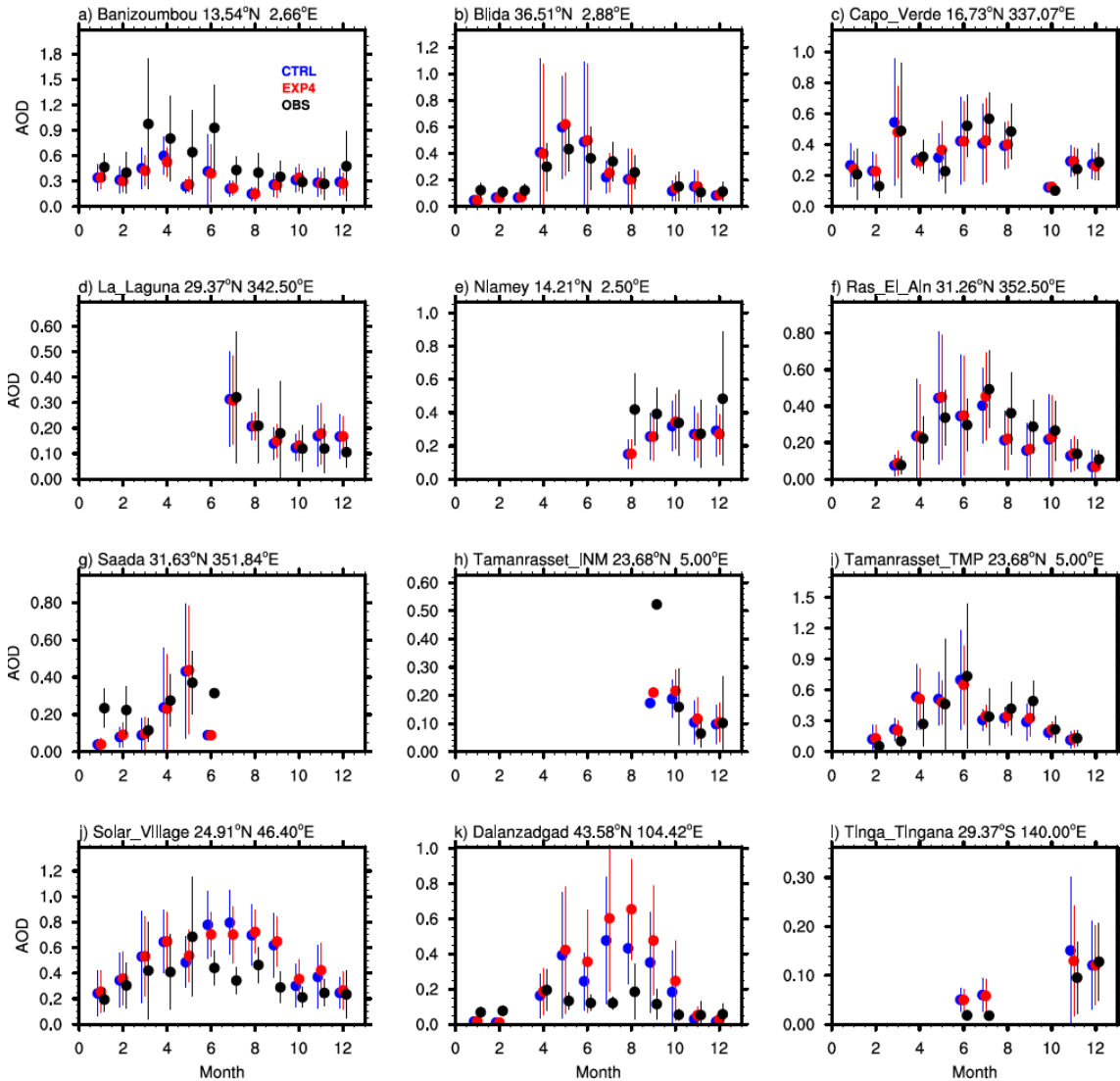


Figure R1.4: As Figure R1.3 but for *coarse mode* AOD.

Comment: In section 5.2 also the impact of the emission changes due to subgrid scale wind variability on radiative forcing is shown. This part is unnecessary and misleading, since the ‘best’ model version would be EXP 4, which is not shown. Radiative forcing by dust aerosol depends not only on dust AOD but also on optical properties of the particles, which add considerable uncertainties. Given these uncertainties and the lack of new information, this part (including Figure 16) should be removed from the paper. Instead more attention should be given to evaluation of the model changes.

Reply: Following the reviewer’s suggestion, we have removed the aforementioned subsection in the revised paper.

Comment: A more important result is provided later in section 5.2. The shift of the frequency of dust events towards smaller but more numerous dust emission events when including the subgridscale parameterisation is quite significant. While it is true that the temporal coverage of aerosol retrievals by polar orbiting satellite instruments provide too little temporal coverage to evaluate the dust emission frequencies, note that are results from geostationary satellites that can provide useful information. E.g., the infrared dust index data for Saharan dust retrieved from the Meteosat SEVIRI instrument provides dust information at 15min intervals (see e.g. Schepanski et al., 2007, GRL).

Reply: We thank the reviewer for the reference. In the revised paper, we have added the following paragraphs and figure in section 5.5, “Dust emission frequency”:

“Ideally it would be nice to use observational data sets to evaluate whether such a shift also makes the simulated emissions more realistic. For example, Schepanski et al. (2007) presented seasonal dust source area maps for the Sahara and Sahel region derived from IR-channel images of Meteosat Second Generation. A quantitative comparison between our simulations and their results is however difficult, because the absolute value of the emission frequency depends strongly on the dust mass flux threshold that is used when identifying an emission event. In the work of Schepanski et al. (2007), dust emission was identified by visually detecting dust plumes, then visually tracing the plume patterns back to their origin by inspecting consecutive images during dust mobilization and transport events. In order to directly compare their maps with our simulations, one would need to implement a satellite simulator in our model, produce the IR-channel images, then apply the same human-involved method of visual dust activation identification. Such an evaluation is impractical in our study; below we limit ourselves to a qualitative comparison with the results of Schepanski et al. (2007).

Maps of seasonal dust emission frequencies in Africa and Asia are presented for CTRL and EXP4 in Fig. 20. Since it is unclear what dust emission flux thresholds the maps of Schepanski et al. (2007) correspond to, we chose a somewhat arbitrary (but low) threshold of $10^{-9} \text{ kg}^{-2} \text{ s}^{-1}$. Fig. 20 indicates that the inclusion of wind SGV generally increases the frequency of dust emission; this is consistent with the PDFs shown in Fig. 19. In addition, EXP4 features enhanced seasonal differences compared to CTRL: wind variability associated with dry convective eddies leads to considerably more frequent dust emission in boreal spring/summer than in autumn/winter.

In terms of geographical distribution, Schepanski et al. (2007). showed seasonal shifts of dust emission patterns in North Africa. In our simulated, however, dust emissions largely occur at the same locations all year round, except in Northwest China where the source regions are larger in spring and summer. The frequency patterns in CTRL and EXP4 are similar, and both differ in the details from the maps of Schepanski et al. (2007). The same turned out to be true when we increased the emission flux threshold to higher values. Our analysis showed that the wind SGV changes the magnitudes of the emission frequency, but does not significantly change the spatial pattern. This is

not surprising since apart from wind speed, the simulated dust emission also depends on other assumptions in the parameterization scheme as well as the surface properties in the model.”

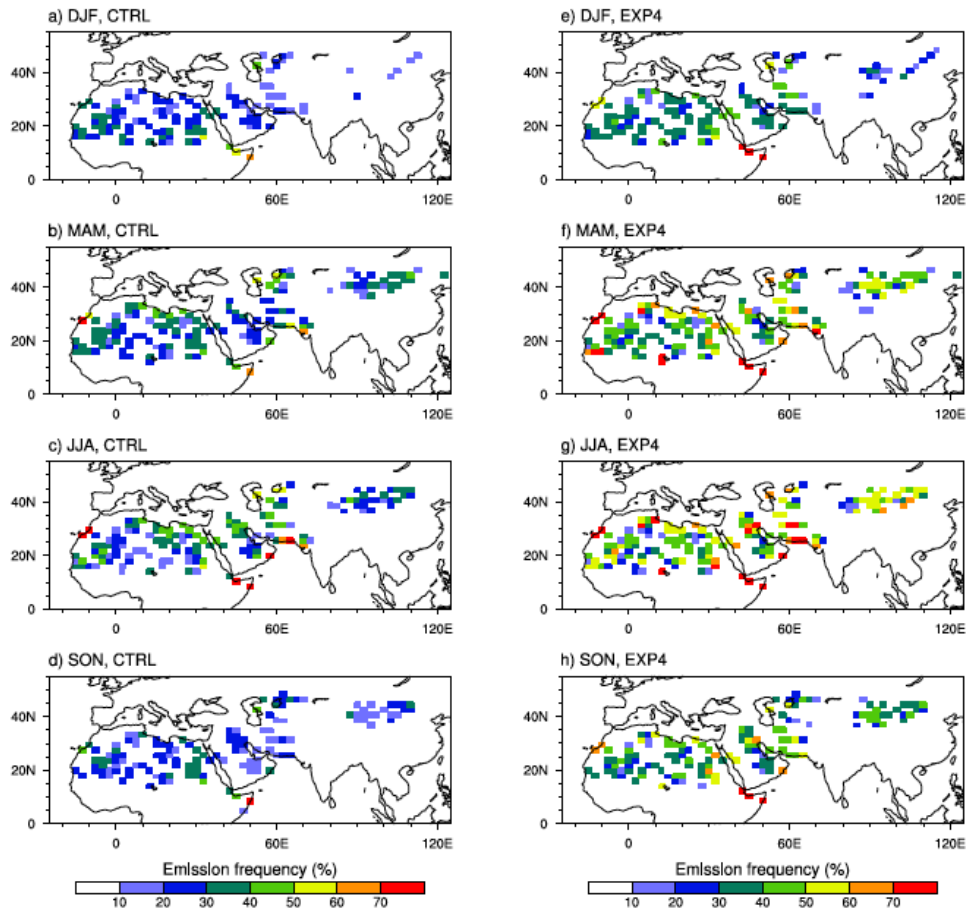


Figure 20. Frequency of occurrence (unit: %) of dust emission fluxes stronger than $10^{-9} \text{ kg}^{-2} \text{ s}^{-1}$ in Africa and Asia in the CTRL simulation (left column) and in EXP4 (right column). Different rows correspond to different seasons: December-January-February (DJF), March-April-May (MAM), June-July-August (JJA), and September-October-November (SON).

Comment: Figure 17 is interesting, here it would be nice if the results could also be shown for larger areas, e.g. for the whole Sahara.

Reply: The figure has been revised as suggested, and copied below. We now show distributions for larger areas in Northwest China, North Africa, and Australia.

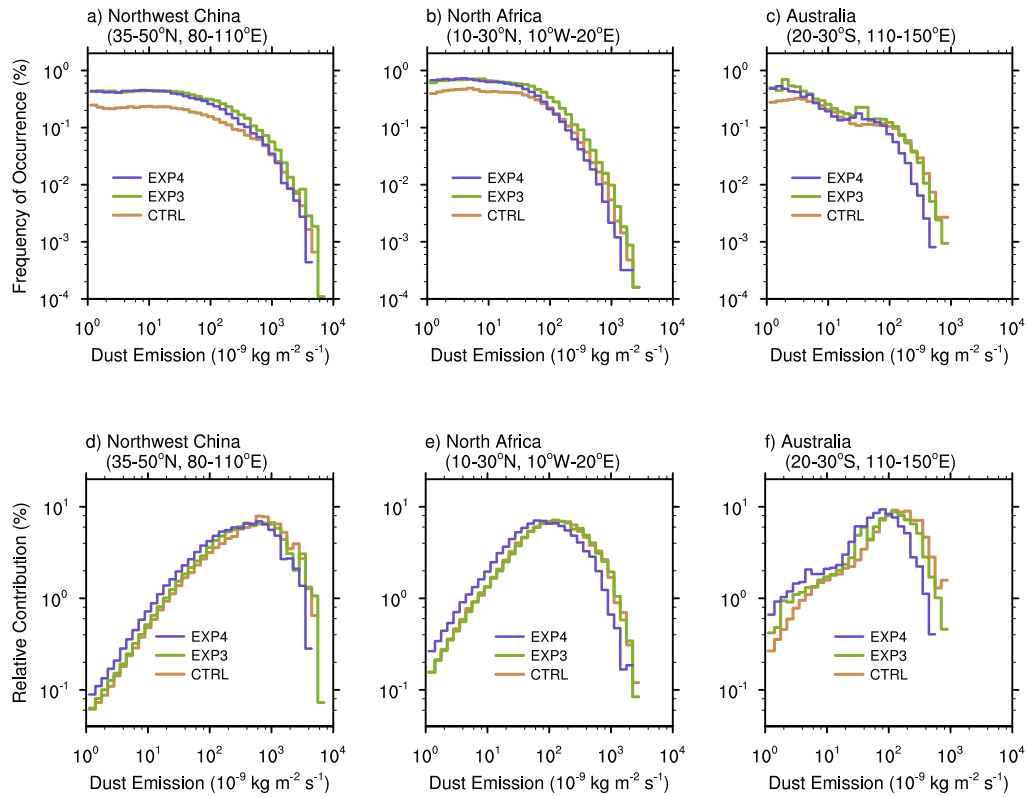


Figure 19. Upper row: frequency distribution of simulated dust emissions in (a) Northwest China, (b) North Africa, and (c) Australia. Lower row: relative contribution of each emission flux bin to the total emission in those three regions. The results were derived from hourly emission fluxes of the year 2006. All grid cells in each region were treated as individual samples.

Comment: Another major concern is that the results of the effects of the subgridscale wind parameterisation are mostly shown by maps of relative changes, particularly in figures 13 and 14. Showing absolute changes would be better at least exemplary, since it would show where the wind modifications actually play an important role for the emissions and AODs.

Reply: For these two figures, we show in the revised paper (1) the emissions and AODs in the CTRL simulation, (2) the absolute differences between EXP3 and CTRL, and (3) the relative differences between EXP3 and CTRL. The new figures are copied below.

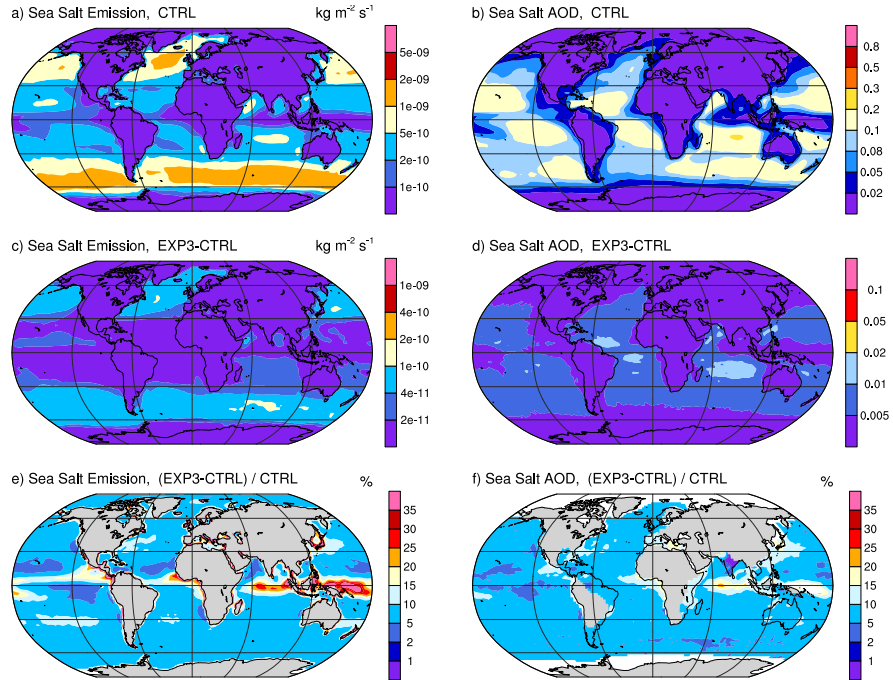


Figure 15. Top row: year 2006 mean sea salt emission flux ($\text{kg m}^{-2} \text{s}^{-1}$) and AOD (unitless, sea salt only) in the nudged CAM5 simulation (CTRL); Second row: differences between EXP3 and CTRL. Bottom row: relative differences between EXP3 and CTRL. In the bottom row, locations that have emission fluxes less than $1 \times 10^{-12} \text{ kg m}^{-2} \text{ s}^{-1}$ or sea salt AOD < 0.01 in the CTRL simulation are masked out.

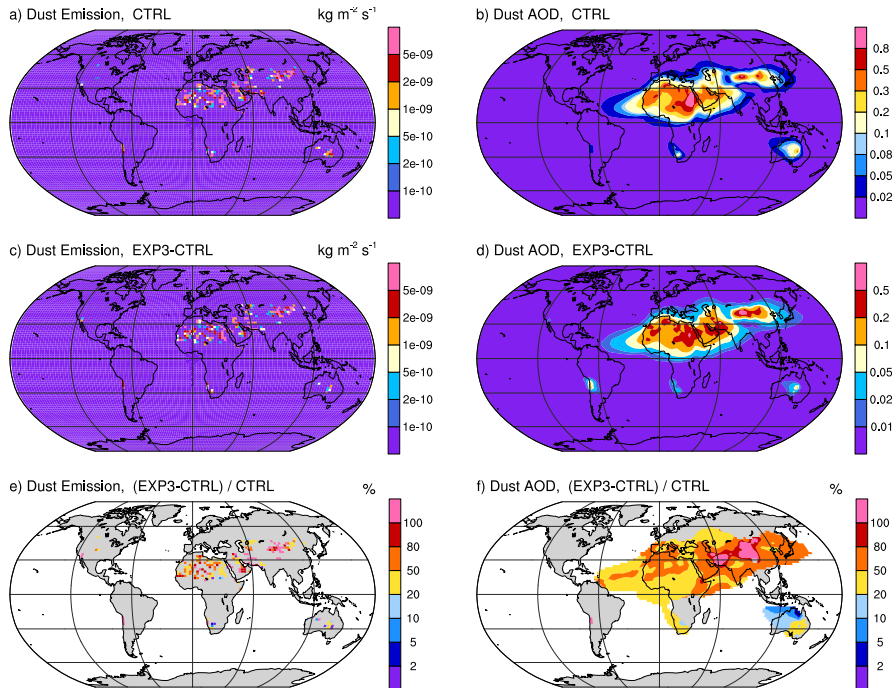


Figure 16. As in Fig. 15 but for dust emission and AOD. The threshold values for masking out differences in the bottom row are $1 \times 10^{-10} \text{ kg m}^{-2} \text{ s}^{-1}$ for emission and 0.01 for AOD.

Comment: And at least for EXP4 maps of emissions and AOD (not differences) should be shown together with the results of the Control simulation to show how emission and AOD patterns change when using the new parameterization.

Reply: We have added the following figure and discussion to the revised manuscript to show the dust emission and AOD maps of EXP4 together with the absolute and relative differences from CTRL. The emission and AOD maps of the CTRL simulation are provided in Figure 16 (copied above in response to the previous comment).

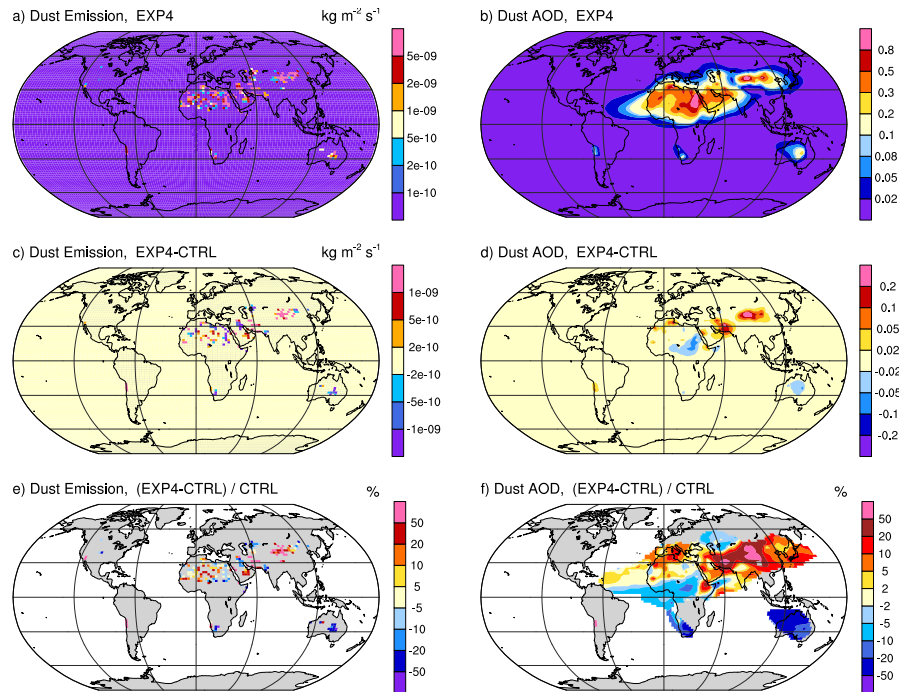


Figure 18. Top row: year 2006 mean dust emission flux ($\text{kg m}^{-2} \text{s}^{-1}$) and AOD (unitless, dust only) in EXP4; Second row: differences between EXP4 and CTRL. Bottom row: relative differences between EXP4 and CTRL. In the bottom row, locations that have emission fluxes less than $1 \times 10^{-10} \text{ kg m}^{-2} \text{s}^{-1}$ or AOD < 0.01 in the CTRL simulation are masked out.

“In Fig.18, annual mean global maps of dust emission and AOD are presented for EXP4. The absolute and relative differences with respect to the default model are also shown. While the geographical distributions are similar in both model versions, taking into account wind SGV then retuning the global mean leads to dust AOD increases in Asia and Northwest Africa, and decreases in Australia and tropical Africa (Fig. 18d and f). A comparison between the emission flux difference in Fig. 18c and e with the wind SGV maps in Fig. 14 suggests that the grid cells with decreased emissions are typically associated with smaller wind variabilities related to unresolved topography, while those grid cells with increased emissions are associated with stronger wind variabilities caused by topography and/or dry convective eddies.”

Minor comments:

Comment: Section 2.4: In the description of the dust emission scheme, please state what the threshold for dust emission is based upon in the scheme (topography, soil type, texture, or anything else?)

Reply: We explained in the discussion paper that in CAM5/CLM, dust emission can occur on bare-ground surfaces in the “vegetated” type of landunits, while glaciers, wetlands, lakes, and urban areas are assumed to not emit dust. In the revised paper, we have added that in the “vegetated” landunits, the threshold friction velocity for dust emission is determined by the size and density of the optimal saltation particles which are assumed to have a diameter of 75 micrometer (Zender et al., 2003). The threshold friction velocity also depends on soil moisture and ambient air density. The detailed formulation can be found in Chapter 10 of the CLM documentation (Oleson et al., 2010).

Comment: Figure 4: not much can be learned from this figure. The differences might be better illustrated by frequency distributions.

Reply: For Figure 4 (sea salt) and Figure 6 (dust), we have added the joint frequency distribution of the relative and absolute errors.

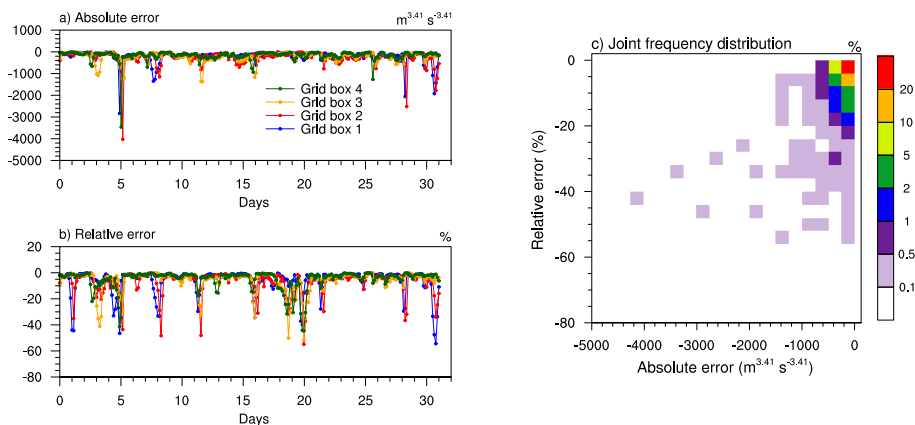


Figure 4. (a)-(b): Time series of the error of $U_{10}^{3.41}$ in the four $225 \text{ km} \times 225 \text{ km}$ grid boxes in the WRF domain over the Southern Ocean (cf. Fig. 1 and Sect. 3). The absolute and relative errors are calculated for Eq. (10) assuming Eq. (11) is the “truth”. (c) Joint frequency distribution of the relative and absolute errors. All the 4 time series shown in panels (a) and (b) are considered as one sample for the calculation.

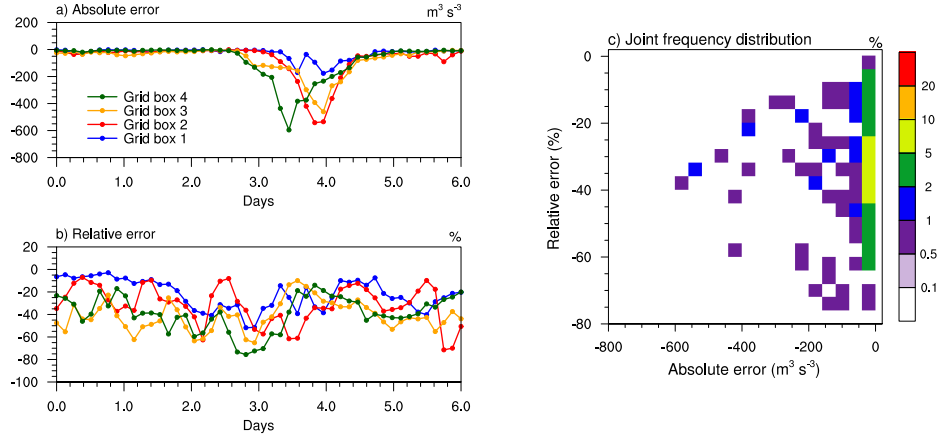


Figure 6. As in Fig. 4 but for the WRF simulation over Western China, and for the error of U_{10}^3 . The errors are calculated for Eq. (12) assuming Eq. (13) is the “truth”.

Comment: Section 4: For the purpose of getting an overview in which area which processes play a role it would be interesting to show maps of σ_d , $\sigma_{U,t}$, $\sigma_{U,m}$, $\sigma_{U,l}$.

Reply: The following figure and text are added to the revised manuscript. When addressing this comment, a bug was found in the calculation of $\sigma_{U,d}$ and $\sigma_{U,t}$ over the ocean. We have fixed the bug and repeated EXP1-4. The major findings still hold, but the relative contribution of dry convective eddies and turbulence over the ocean is changed. The text, figures and tables related to EXP1-4 have been corrected in the revised manuscript.

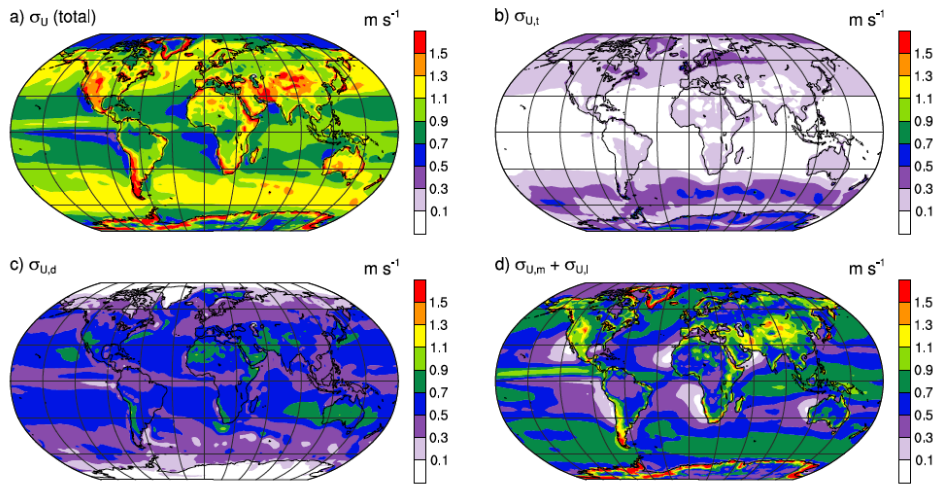


Figure 14. Annual mean sub-grid standard deviation of surface wind speed in CAM5: (a) total (Eqn. 19), (b) neutral/stable turbulent mixing (Eqn. 20), (c) dry convective eddies (Eqn. 21), (d) moist convective eddies over the ocean (Eqn. 23–24) and mesoscale flow over land (Eqn. 27).

“5.1 Online calculated sub-grid scale wind variability

Annual averages of the estimated sub-grid standard deviation of surface wind speed in CAM5 are presented in Fig. 14a, and the individual components are shown in Fig. 14b-d. Strong SGVs are associated with complex topography, mid-latitude storm tracks, the trade winds, and tropical convection. Over the ocean, moist convective eddies are the most important contributor to wind SGV in the tropics (Fig. 14d), while dry convective eddies are the main contributor in the trade wind regions and above warm ocean currents (Fig. 14c). Over the continents, strong wind variabilities are associated with sub-grid topography and dry convective eddies (Fig. 14c-d). The impact of neutral/stable turbulent mixing is seen mainly in middle- and high-latitude regions (Fig. 14b).

Since the empirical parameterizations for $\sigma_{u,m}$ and $\sigma_{u,l}$ were derived from the ECMWF analysis, the wind SGV in Fig.14d agree reasonably well with the diagnostic results shown in Fig.2f for the ECMWF data. The discrepancies over the ocean are attributable to fitting error and differences in the simulated precipitation rates in the two models. Over the continents, the discrepancies are likely caused by the different grid-box mean winds, and the use of a time-independent coefficient D.”

Comment: Section 4.2.3.: Using WRF results, the authors test if the subgridscale variability for the ECMWF 15-km wind fields is appropriate to represent the ‘real’ variability. The WRF model is used at 3 km resolution where usually convection does not need to be parameterized. To test the oceanic surface winds, a test was performed at a location in the southern Pacific. The authors mention that they did not perform such a test in the tropical ocean where major differences can be expected due to strong convective activity. They argue that the sea salt emissions from that regions would weak so that it is not important to test the performance of the 15-km fields there. However this is an implication from computations that neglect subgrid scale wind variability, and not necessarily confirmed by Fig. 2. This problem should be should be discussed

Reply: We have added discussions at two places in the revised paper.

At the end of Section 4.2.3:

“Such a comparison is not included in this paper because as discussed later in Sect. 5.3, CAM5 simulations indicate that sea salt emission fluxes are very low in the tropics; even with Redelsperger's formula which gives stronger wind variability than our fitting does, the absolute increases in sea salt emission and loading remain negligible when compared with higher latitudes.”

In Section 5.3:

“An additional sensitivity experiment was conducted using the formula of Redelsperger et al. (2000) for the moist convective eddies. The strongest enhancement of sea salt

emission exceeded 100% in the ITCZ, while the resulting emission fluxes remained a factor of 5-10 weaker than in the storm tracks, and the increases in sea salt AOD were generally below 50%. Although the Redelsperger et al. (2000) formula leads to higher wind SGV than our empirical fitting derived from the ECMWF analysis, the impact on the simulated sea salt emission and AOD is still small in terms of global mean and geographical distribution."

Comment: Section 4.2.4, Figure 10: Since the $\sigma_{U,l}$ is inversely related to the coefficient C, Figure 1 should depict $1/C$ rather than C, since this would provide a measure of the subgrid scale variability. Also, in Figure 10 the letters indicating the locations of the time series shown in Figure 11 should be indicated next to the appropriate boxes.

Reply: We have revised the figure so that it shows $1/C$, and updated Eqns. (25)–(27) so that they use a new parameter $D=1/C$. The locations of the time series are added to the figure (see below).

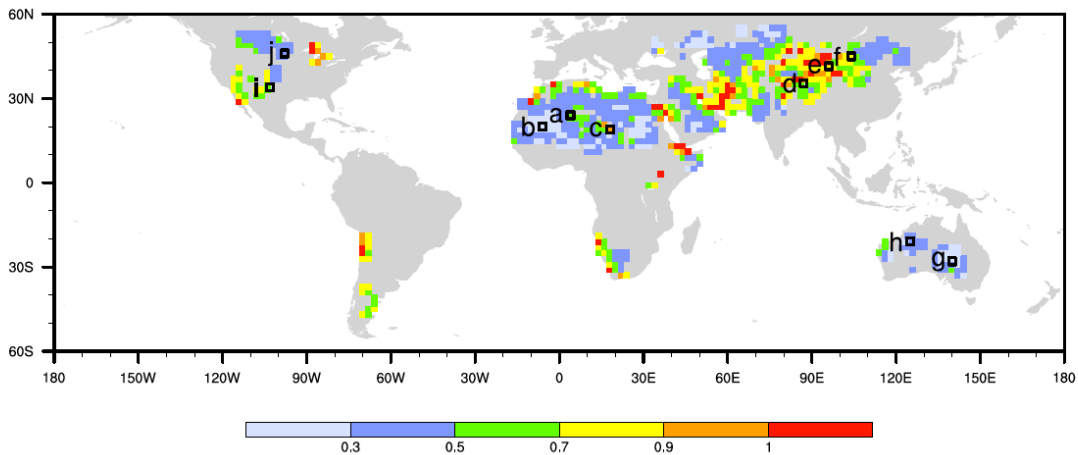


Figure 10. Geographical distribution of the coefficient D (unitless) derived for a $2^\circ \text{ lat} \times 2^\circ \text{ lon}$ GCM grid using the ECMWF 15 km analysis of the year 2011 and Eq. (26). The locations with no results are either covered by land ice or lake, or associated with leaf area indices (LAI) larger than 0.3 throughout the year, thus cannot have dust emission according to the parameterization of Zender et al. (2003) and the land surface characteristics data used in the CAM5 simulations in this paper. The black boxes correspond to the panels in Fig. 11 in which time series of sub-grid wind variability are analyzed.

Comment: Section 4.2.4 : As above for the ocean, the applicability of the 15-km ECMWF wind fields to offer a good measure of wind speed variabilities used to compute dust emissions are tested for a location in the Taklamakan region with a few days of a 3-km WRF simulation. The authors find a good agreement in that region and argue that the differences in the flatter terrain in the Sahara are expected to be minor since the orography would have a small effect. However, note that e.g. Marsham et al. (2011) found considerable subgrid scale wind activity during summer conditions in the Sahara due to wet convective activity using regional

model study at 4 km grid resolution. Neglecting this process will cause an underestimate of subgrid scale surface winds, which should be discussed in the text.

Reply: We removed the original statements on resolution issue over flatter terrain, and added the following discussion:

“It should be mentioned that the reference solution here has limitations in terms of the spatial and temporal coverage, and the horizontal and vertical resolutions. Physical mechanisms of dust emission in the real world and their representation in numerical models are highly complex. For example, Marsham et al. (2011) showed that models with parameterized or resolved convection can give different timings of summer dust uplift in West Africa. The parameterization of wind SGV presented in this paper is very simple and empirical. Process-based representation of different dust emission mechanisms is a topic for future study.”

Comment: Section 4.3: To illustrate the implementation of the subgrid scale processes in the model a flowchart would be helpful.

Reply: A flowchart is added in the revised manuscript.

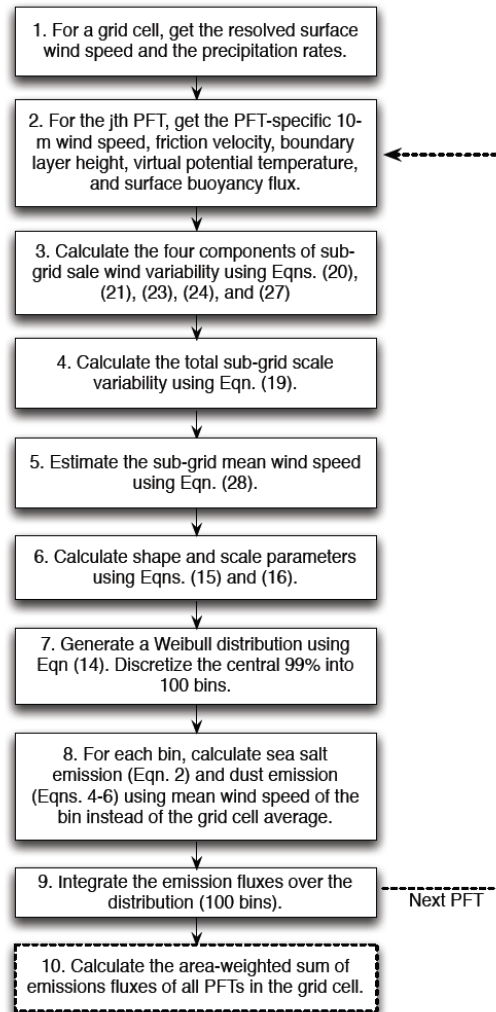


Figure 13. Flowchart illustrating the implementation of wind-distribution-based sub-grid emission calculations in CAM5. Dashed lines indicate steps that are only relevant for the dust emission calculation.

References:

Schepanski, K., I. Tegen, B. Laurent, B. Heinold, and A. Macke (2007), A new Saharan dust source activation frequency map derived from MSG-SEVIRI IR-channels, *Geophys. Res. Lett.*, 34, L18803, doi: 10.1029/2007GL030168

Marsham, J, Knippertz P; Dixon N; Parker DJ; Lister GMS (2011): The importance of deep convection for summertime dust uplift over West Africa, *Geophysical Research Letters*, 38, . doi: 10.1029/2011GL048368

These references have been added to the revised paper.